



Evaluating the effectiveness of self-cleaning products applied on external thermal insulation composite systems (ETICS)

Ana Sofia Silva, Giovanni Borsoi , João Luís Parracha, Inês Flores-Colen, Rosário Veiga, Paulina Faria, Amélia Dionísio

Received: 4 July 2021 / Revised: 18 January 2022 / Accepted: 22 January 2022
© American Coatings Association 2022

Abstract External thermal insulation composite systems (ETICS) have been extensively applied on building façades with the aim of implementing the thermal and aesthetical properties of the building envelope. However, the formation of stains and deposition of particulate matter is often observed in the surface of these systems. The use of multifunctional products with self-cleaning properties can reduce surface anomalies and thus enhance the durability of ETICS. This study aims at evaluating the effectiveness of three protective coatings with self-cleaning additives (i.e., TiO₂ nanoparticles), when applied on the surface of ETICS. Three different stains (rhodamine, methylene blue and silver paint aerosol) were applied on the ETICS finishing coat, evaluating the removal of these stains after exposure to natural (solar radiation) light source. The surface properties (compactness, hardness, roughness, gloss, and color) of the ETICS were

evaluated prior and after sun exposure. Results showed that the application of the three products lead to a modification of the surface properties (compactness, hardness, gloss, roughness) of the ETICS specimens, and sensibly enhance the self-cleaning, hydrophobic and aesthetical properties of the ETICS.

Keywords ETICS, Protective coatings, Self-cleaning additives, Photocatalysis

Introduction

External Thermal Insulation Composite Systems (ETICS), also identified as EWI in the UK and EIFS in the USA, have been widely used as constructive solutions in the last decades, with the aim of improving the energy efficiency of the built environment by reducing the thermal losses throughout the external walls.^{1, 2} These composite systems generally include a thermal insulation layer and a rendering system, i.e., a basecoat reinforced with a glass fiber mesh and a finishing coat. The latter, which generally consists of a paint or a thick plastic coating, is constantly exposed to weathering and anthropic factors, which can affect the durability of the ETICS.

In fact, several anomalies (e.g., stains, discoloration, biological growth) can appear on the finishing coat of the ETICS over time, both in new constructions and retrofitted buildings.^{1, 3, 4} The biological susceptibility of ETICS is mostly related to the physical-chemical properties of the finishing coat (e.g., moisture content, temperature, surface roughness, pH, content of organic additives),^{5, 6} whereas the formation of stains and further surface anomalies can be also favored by the deposition of environmental pollutants.⁷ In order to tackle this problem, the application of multifunctional products with self-cleaning properties can be a useful

A. S. Silva, I. Flores-Colen, A. Dionísio
DECivil, Instituto Superior Técnico, University of Lisbon,
Av. Rovisco Pais, 1049-001 Lisbon, Portugal

G. Borsoi (✉), J. L. Parracha, I. Flores-Colen,
P. Faria
CERIS, Instituto Superior Técnico, University of Lisbon,
Av. Rovisco Pais, 1049-001 Lisbon, Portugal
e-mail: giovanni.borsoi@tecnico.ulisboa.pt

J. L. Parracha, R. Veiga
Buildings Department, LNEC, National Laboratory for
Civil Engineering, Av. do Brasil, 101, 1700-066 Lisbon,
Portugal

P. Faria
DEC, NOVA School of Science and Technology, NOVA
University of Lisbon, 2829-516 Caparica, Portugal

A. Dionísio
CERENA, Instituto Superior Técnico, University of Lisbon,
Av. Rovisco Pais, 1049-001 Lisbon, Portugal

tool to provide a further protective layer and enhance the aesthetic durability of the system.⁸

Self-cleaning products have been used for numerous applications in building materials, such as glazed facades, coatings and tiles, and other decoration materials.^{9, 10} The self-cleaning mechanism is based on the photocatalytic activity of specific additives, such as (microstructured or nanostructured) titanium oxide (TiO₂) or zinc oxide (ZnO) nanoparticles,¹¹ semiconductor materials that can efficiently remove organic pollutants and dyes.¹²

Photocatalysis is a physical-chemical process that occurs when ultraviolet photons, with energy higher than the material band gap, are absorbed in the semiconductor materials.¹³ When the photon is absorbed by the material, the electrons move from the valence band (BV) to the conduction band (BC),^{7, 14, 15} causing a charge imbalance and originating a reactive hole (h⁺) and an electron (e⁻). The latter participate in the photocatalytic process by chemically reacting with molecular oxygen (O₂) present in the environment, forming superoxide radical anions (O₂⁻), and with water present in the environment, forming hydroxyl (OH⁻) radicals.^{13, 16} The rather reactive free radicals work together to decompose environmental pollutants, organic compounds or particulate matter, forming water-soluble compounds that easily runoff from the substrate.¹⁴ Furthermore, free radicals can also penetrate and destroy cellular membranes, inhibiting biological growth.¹⁷⁻¹⁹

In this study, the behavior of three protective coatings with self-cleaning properties was evaluated when applied on the surface of the ETICS. As reported in previous studies^{12, 20-24} and also in accordance with a European standard,²⁵ the photocatalytic effect of these materials was analyzed by evaluating the degradation of specific pigments (e.g., rhodamine, methylene blue).

Materials and methods

ETICS specimens

ETICS specimens consist of a molded expanded polystyrene (EPS) insulation board (with a thickness of ~ 40 mm), a rendering system with a cement-based basecoat and a glass fiber mesh (2–2.2 mm thick), and an acrylic-based finishing coat (0.5–0.7 mm thick) with hydrophobic and biocide properties (Fig. 1).⁶ The finishing coat, obtained by applying a key-coat and a paint, contains acrylic additives and biocides (e.g., terbutryn, isothiazole), as well as additives (e.g., TiO₂, ZnO) used as white pigment and/or photocatalytic additives. The ETICS have European Technical Approval (ETA) and, thus, adequate durability and suitable performance, considering the requirements of the EAD 040083-00-0404.²⁶

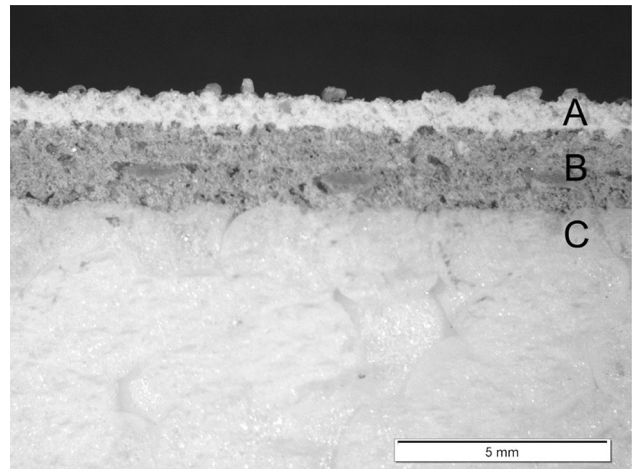


Fig. 1: Cross section of the ETICS specimens: (A) acrylic-based finishing coat; (B) cementitious basecoat; (C) EPS board

Prismatic specimens with dimensions of 150 mm × 150 mm and 42.5–43 mm thickness were cut from larger ETICS board specimens and used during the tests.

Protective coatings

Three waterborne protective coatings (identified as P1, P2, and P3) were used. Some properties of these products are listed in Table 1.

P1 and P3 are commercially available acrylic-based products, which present TiO₂ and ZnO (which can be used as white pigments or photocatalytic additive), calcium carbonates (white pigment and filler) and biocide additives in their composition. P3 also contains a low percentage of other acrylates (i.e., diisobutyrate, butyl acrylate, methyl methacrylate), whereas P1 presents zinc pyrithione (biocide additive). It should be noted that the amount of TiO₂ (rutile) in the composition of P1 and P3 is comprised between 10% and 25% in mass. On the other hand, P2 is an experimental product, thus its pH and dry residue were also evaluated through laboratory tests.

Application protocol

Three sound ETICS specimens (reference – P0) and three ETICS specimens with each of the three protective coatings (P1, P2, P3) were tested. The products were applied threefold by brushing, applying two coats of each protective coatings in orthogonal directions (Fig. 1, Table 1). The first coat was diluted at 10% with distilled water, in compliance with the manufacturer instructions. A drying time of 24 h among coats was considered to guarantee the complete evaporation of the aqueous solvent.

Table 1: Physical features and amount of product used in the application of the protective coatings

Product identification	pH	Density (g/cm ³) at T = 20°C	Dry residue (g/l)	Amount of product per application (l/m ²)*
P1	8.5 *	1.34 ± 0.05*	737	1st coat: 0.13
P2	8.4	1.32 ± 0.06	718	2nd coat: 0.12
P3	8.5 *	1.30 ± 0.03*	729	

*In accordance with technical data sheets

Surface properties

Ultrasonic pulse velocity was determined using the ultrasonic tester Steinkamp model BP-7, and adopting the indirect transmission method, as described in FE Pa 43.²⁷ Two piezoelectric sensors were coupled on the same face of the specimen to measure the transit time for the ultrasonic pulse and 10 measurements at 1 cm interval were carried out on each specimen, with 3 repetitions, and considering the average value. The point-contact transducers used have a resonance frequency of 45 kHz, with measuring range from 0.1 μs to 9999.9 μs and accuracy of ± 0.1 μs. The ultrasonic pulse velocity was calculated from the ratio of travel distance to transit time of the wave through the specimens, to facilitate a comparison between the compactness and elastic properties of the treated and untreated sound specimens, and eventually the presence of microcracks or discontinuities.

Surface hardness was defined using a durometer Shore A, according to ASTM D2240.²⁸ Values were recorded in nine different spots along the surface of the specimens, considering the average value.

The surface gloss was assessed using a Rhopoint Novo-Gloss Lite glossmeter, in accordance with ASTM D6578,²⁹ considering a measurement geometry of 60°. Specimens were analyzed in nine different spots, as in the case of the hardness measurements, considering the average value.

Surface roughness was measured with an Elcometer 223 surface profile gauge. This device can measure the peak-to-valley value of a surface up to 2 mm, with a resolution of 0.001 mm. Nine measurements were collected in different spots of each specimen, and the average value considered.

The water contact angles were measured by sessile drop shape analysis technique. This test is based on the variation of the interface free energy (area/water drop) and is carried out by dropping 4 ± 0.4 μl of water with a micropipette on the specimen. The images were obtained by a video camera (JAI CV-A50, Spain), mounted on a microscope Wild M3Z (Leica Microsystems, Germany), and analyzed using MATLAB. The contact angle is measured according to equation (1) and assuming that the droplet has the shape of a spherical segment:

$$\theta = 2\arctan \frac{2h}{a} \quad (1)$$

where h is the height of the apex of the micro-drop and a the micro-drop diameter, respectively. The mean value of four static contact angle measurements was considered.

Morphological and microstructural characterization

Optical microscopy was used to evaluate the surface of the untreated and treated ETICS specimens, in order to detect possible microstructural modifications of the finishing coat after the application of the protective coatings. The surfaces of the specimens were observed using a stereomicroscope Olympus SZH-10 equipped with an image acquisition system Olympus SC-30 and with the software Olympus LabSens.

Additionally, morphological and elemental analysis of untreated and treated specimens were carried out by scanning electron microscopy (SEM). A SEM Hitachi S-2400, working at an acceleration voltage of 20 kV, and coupled with an Oxford Inca X-Sight energy dispersive X-ray spectrometer, was used. Samples were sputtered with an Au-Pd (80:20) film before analysis.

Self-cleaning test

This test aims at analyzing the self-cleaning effectiveness of the three protective coatings by evaluating the degradation of three different stains (rhodamine B, methylene blue, aerosol spray paint) over time, when applied on the surface of the ETICS specimens and exposed to sunlight.

Water-based solutions of rhodamine B (RhB), a chemical compound based on functionalized dyethylammonium chloride (C₂₈H₃₁ClN₂O₃), and methylene blue (MB), a dye based on methylthionium chloride (C₁₆H₁₈ClN₃S), were prepared, with concentration of 0.05 g.l⁻¹. These solutions were applied by micropipette (0.5 ml/stain) on the surface of the specimens, forming stains with ≈ 2 cm diameter in accordance with UNI 11259²⁵ (Fig. 2b). Two different stains of each solution were applied on the ETICS specimens (Fig. 2c).

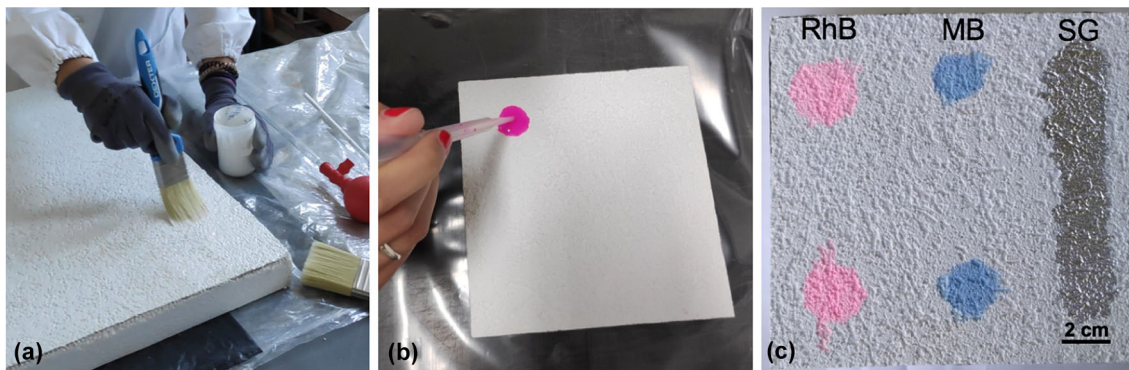


Fig. 2: (a) Application of protective coating on ETICS board; (b) Application of rhodamine B (RhB) stains on ETICS specimen; (c) Stains of RhB, methylene blue (MB) and silver aerosol spray (SG) on a ETICS specimen

Furthermore, a silver chrome aerosol spray paint (RAL 7001, Montana Colors S.L., currently used for graffiti) (SG), was also applied on the ETICS specimens ($\approx 10 \times 2$ cm stripe) (Fig. 2c). This graffiti paint has an acrylic-based binder (alkyl and polyester resins) and in addition to carbon, contains aluminum (19.43%) and, to a significant lower extent, iron and zinc.³⁰

For the self-cleaning test, the specimens were exposed outdoor in Lisbon, Portugal (38°45'31"N; 9°8'29"W; Altitude – 95 m), during one month (from 19 June to 18 July 2020). Specimens were placed on a rack, in a steel support at 45° of inclination and South-oriented, with the intention of maximizing solar exposure.^{31, 32} During the exposure time the temperature ranged between 16°C and 35°C (average 22.4°C) and the relative humidity (RH) between 26% and 94% (average 61%), without rainy days, according to the Portuguese Institute for Sea and Atmosphere (IPMA).³³ Furthermore, the mean dose of solar radiation received by the specimens (during the day, i.e., between 6 am and 8 pm) was 2070 kJ/m² per hour.³³ Specimens were exposed to solar radiation with an average light exposure of 12 h/day (total of 360 h), thus receiving a dose around 745 MJ/m² during this month of exposure. Specimens were covered by a plastic tarp during the night time, in order to avoid condensation phenomena (at the dew point) and thus possibly affect the stability of the stains. If considering that around 5% of solar terrestrial radiation is UV radiation, being 95% UV-A rays,^{34, 35} the average UV-A dose received at surface is thus 103,5 kJ/m² per hour.

A Minolta CR-410 chromameter was used to evaluate the color coordinates (L^* , a^* , b^*) of the specimens before and after sun exposure.³⁶ In the CIELAB color system, the value L^* corresponds to the lightness, which ranges from 0 (black) to 100 (white). The a^* and b^* values characterize the chromatic coordinates of red-green ($+a^*$ indicates red and $-a^*$ green) and yellow-blue ($+b^*$ corresponds to yellow and $-b^*$ to blue), respectively. The measurements were performed in specular component included mode (SCI), using the illuminant D_{65} (which corresponds to average daylight illumination, including ultraviolet radiation) at obser-

ver angle of 2° and a 50 mm diameter area of measurement.

The chroma or color saturation (C_{ab}^*) was obtained according to equation (2).

$$C_{ab}^* = (a^{*2} + b^{*2})^{0.5} \quad (2)$$

The total color variation, ΔE^* , was also obtained by equation (3).

$$\Delta E_{ab}^* = (\Delta L^{*2} + \Delta a^{*2} + \Delta b^{*2})^{0.5} \quad (3)$$

ΔL^* , Δa^* and Δb^* represent the difference of L^* , a^* and b^* values at the end and beginning of the test, respectively.

In order to evaluate the photo-induced decomposition of RhB and MB stains, the photocatalytic decoloration of the stains (D^*) was calculated, adapting a methodology from Munafò et al.³¹ as follows:

$$D^*(t) = \frac{|C^*(t) - C^*(\text{RhB})|}{|C^*(\text{RhB}) - C^*(0)|} \times 100 \quad (4)$$

where $C^*(0)$ is the initial chroma value of untreated and treated specimens, as defined in equation 2, $C^*(\text{RhB})$ is the average chroma value per specimens after the application and drying of rhodamine B on the specimens, and $C^*(t)$ is the chroma intensity after sun exposure.

Results

Surface properties

Table 2 shows the results of the mechanical, optical and hygric properties of treated (coated with the protective coatings) and untreated (reference) ETICS specimens.

Treated specimens present higher values of P-wave velocity when compared to the untreated specimens.

Table 2: Mean values and standard deviations of the ultrasonic propagation speed (S_p), surface hardness, surface gloss, surface roughness, and contact angle (θ) of the untreated (P0) and treated (P1, P2, P3) ETICS specimens

Specimen	S_p (m/s)	Surface hardness (Shore A)	Gloss (GU)	Roughness (mm)	θ ($^\circ$)
P0	2016.1 \pm 32.5	79.00 \pm 6.33	1.30 \pm 0.06	0.774 \pm 0.142	56.30 \pm 5.40
P1	2126.1 \pm 78.7	80.70 \pm 4.86	1.75 \pm 0.06	0.690 \pm 0.038	36.65 \pm 1.69
P2	2111.1 \pm 23.1	84.07 \pm 1.00	1.69 \pm 0.09	0.573 \pm 0.036	31.71 \pm 4.66
P3	2096.4 \pm 31.0	83.11 \pm 2.78	1.68 \pm 0.03	0.657 \pm 0.018	62.75 \pm 4.66

This variation is higher in P1 (5.5%) and slightly less pronounced in P2 and P3 (4.7% and 4%, respectively). In fact, the P-wave velocity in a solid material depends on several features such as the density and elastic properties of the material. Furthermore, each phase that composes the material contributes to the final P-wave velocity proportionally to its own P-wave velocity and volume. These results indicate that all products contribute to increase the compactness of the finishing coat of the ETICS.

The latter results are confirmed by the surface hardness test, which showed an overall hardness trend increase of the ETICS with the application of the protective coatings. Treatment P1 slightly increased the surface hardness (2.2%), if compared to the untreated specimen P0, whereas a higher increase was observed for P2 and P3 (6.4% and 5.2%, respectively). These results indicate that the application of the protective coatings slightly increases the surface resistance of the ETICS solution.

Concerning the contact angle values, ETICS surfaces coated with P3 present the highest θ value (62 $^\circ$), with an increase of 11.4% compared to the untreated specimens (56 $^\circ$). The reduction of the wettability of P3 specimens can be attributed to the inclusion of further hydrophobic acrylic-based compounds (i.e., diisobutylate, butyl acrylate, methyl methacrylate), when compared to the other treatments. On the other hand, P1 and P2 have a decrease of the contact angle (34.9% and 43.7%, respectively) when compared to the reference P0. P1 is a generic product with no specific water-repellent properties stated in its technical data sheet. The inclusion of a significant amount of non-polymeric additives, such as fillers, inorganic additives or pigments, if compared to P3, confer hydrophilic properties to the substrate, explaining the θ decrease.³³ However, none of the surfaces gained hydrophobic features ($\theta > 90^\circ$) after the application of the products, in agreement with previous research.³⁷

The surface gloss slightly increased with the application of the products, when compared to the untreated specimens. Treatments P2 and P3 present similar gloss values, slightly less bright when compared to treatment P1 (+ 34.8% if compared to the reference). This latter value can also be attributed to the addition of submicrometric TiO₂ particles, which have considerably higher refractive index, if compared to

microstructured particles; it was reported that electromagnetic resonance between nanoparticles and light induce an increase of the diffraction, and thus higher refractive index.⁷

The treatments also induced a roughness decrease and homogenization of the surface, if compared to the reference P0. The latter has significantly higher standard deviation and thus more heterogeneous surface. When compared to the reference specimens, the roughness decreased in the case of P2 (26%), and with less extent in the case of P1 and P3 (10.8% and 15.1%, respectively).

Morphological and microstructural analysis

The application of the protective coatings generally provides a homogenization of the treated surface (Fig. 3), as confirmed also in the previous section (as for example in terms of surface roughness), and slightly whiter surfaces a naked eye. The latter effect is quantified by colorimetry in “Self-cleaning test” section. P1 and P2 induced a slightly more homogeneous film, possibly due to their higher content of inorganic additives, compared to P3, which showed some lacunae (Fig. 3d).

SEM-EDS analyses confirmed that the treated substrates are more compact and homogeneous (Figs. 4c–4e), if compared to the reference (Fig. 4a); EDS spectra showed that the finishing coat of the untreated ETICS presents relevant percentages of calcium, possibly associated with CaCO₃ (used both as filler and pigment), and TiO₂, used as white pigment and/or photocatalytic additive (Fig. 4b). Among the two commonly found polymorphs of TiO₂ (anatase and rutile), rutile TiO₂ pigments are generally preferred in coatings due to their higher light scattering, as well as stability and durability, if compared to anatase pigments.³⁸ However, it was reported that anatase has higher photocatalytic activity, if compared to rutile.^{19, 39} No relevant amount of ZnO, which can also exhibit photocatalytic features, was detected.

Furthermore, relevant amounts of silica and aluminum are attributed to the siliceous aggregate, generally used in the finishing coat in order to get some roughness, and to the paint composition. In fact, the addition of alumina and silica can help in the

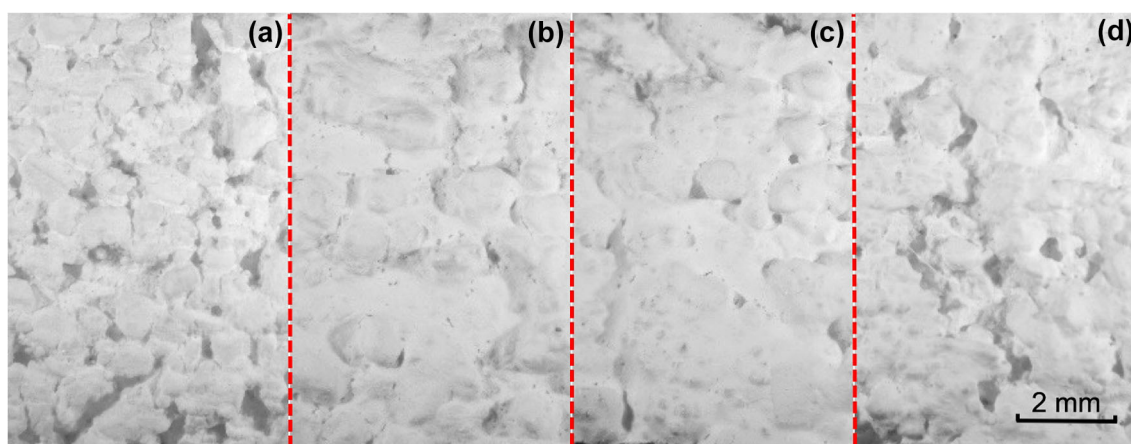


Fig. 3: Microphotographs of (a) untreated system, and system with applied (b) P1, (c) P2 and (d) P3 protective coatings

formulation of paints, providing, e.g., proper dispersibility in water, hiding power efficiency, and higher durability to discoloration by heat and/or photoreduction.³⁸ Furthermore, low amounts of sodium and magnesium were also detected. $\text{Mg}(\text{OH})_2$ can be used as filler or pigment extender. Magnesite and aluminum oxide are also known for being flame retardant additives.³⁸

On the other hand, the treated surface shows considerably higher amount of Ti, especially in the case of P1, if compared to the reference; a reduction of the amount of Ca, Si and Al is observed, mostly in the case of P1, whereas specimens P2 and P3 exhibit intensities of Ca, Si and Al peaks similar to those of the reference, and a higher amount of Mg. When comparing the products, it can be observed that P1 and P2 present higher amounts of prismatic to hexagonal particles in the range 50–250 nm, with relevant molecular weight (i.e., brighter color in the EDS spectra), identified as cluster of submicrometric TiO_2 particle (Fig. 4d). Conversely, specimen P3 presents more relevant amount of rounded to spherical particles, with very similar particle size (≈ 100 nm), which can be attributed to acrylate (e.g., methyl methacrylate) (Fig. 4e).⁴⁰

Self-cleaning test

The chromatic coordinates of the three stains (rhodamine B, RhB; methylene blue, MB; and aerosol spray paint, SG) applied on the ETICS surfaces were evaluated prior and after the exposure to solar radiation.

A complete degradation of the RhB and MB stains in the treated specimens was macroscopically observed after 12–13 days (144–168 h) of sunlight exposure (Fig. 5), whereas no apparent modification of the stain of the aerosol spray paint was observed for all the protective coatings.

Color characterization tests with chromameter allowed to obtain the lightness (L^*) and chroma (C_{ab}^*), as specified in “[Morphological and microstructural characterization](#)” section and shown in Fig. 6. It can be noticed that the treated specimens (P1, P2 and P3) have considerably higher lightness, if compared to the untreated specimen (P0), after sunlight exposure.

When observing the variation of photocatalytic decoloration of the stains (D^*), it can be noticed a $D^* \approx 97\%$ of the RhB stain in the case of P1 after the sunlight exposure (Fig. 6a). This variation is related to the decrease of the CIELAB coordinate a^* to a value close to zero (-0.08 ± 0.02), which corresponds to an almost perfect white. Similar trends were observed in the case of protective coatings P2 and P3, with D^* reduction of the RhB stain in the range ≈ 91 – 95% , again related to the almost zero going of the chromatic coordinate a^* .

It is worth noting that the untreated specimen P0 also presents a significant L^* increase and D^* variation, which can be attributed to the presence of TiO_2 in the finishing coat of the system (without protective product), as seen in “[Morphological and microstructural analysis](#)” section. However, all protective coatings had a more significant color change than P0, especially in the case of RhB stain (Figs. 6a, 6b).

Concerning MB stain, a similar trend is observed in the treated specimens after sunlight exposure, with a significant photocatalytic decoloration in all cases (87–90%). Positive values of the chromatic coordinate b^* were observed, thus, a shift from slightly bluish to whitish (with a tone of yellow) color is registered (Fig. 6c).

Results are in agreement with the values registered for the RhB stains, when compared to that of the MB stains. It should be noted that, as in the case of the RhB stain, the D^* value of the MB stains also decreased in the case of P0 after sun exposure. However, the specimens with the protective products have higher color variation than P0 (Fig. 6b), when compared to the finishing coating of the ETICS, confirming the

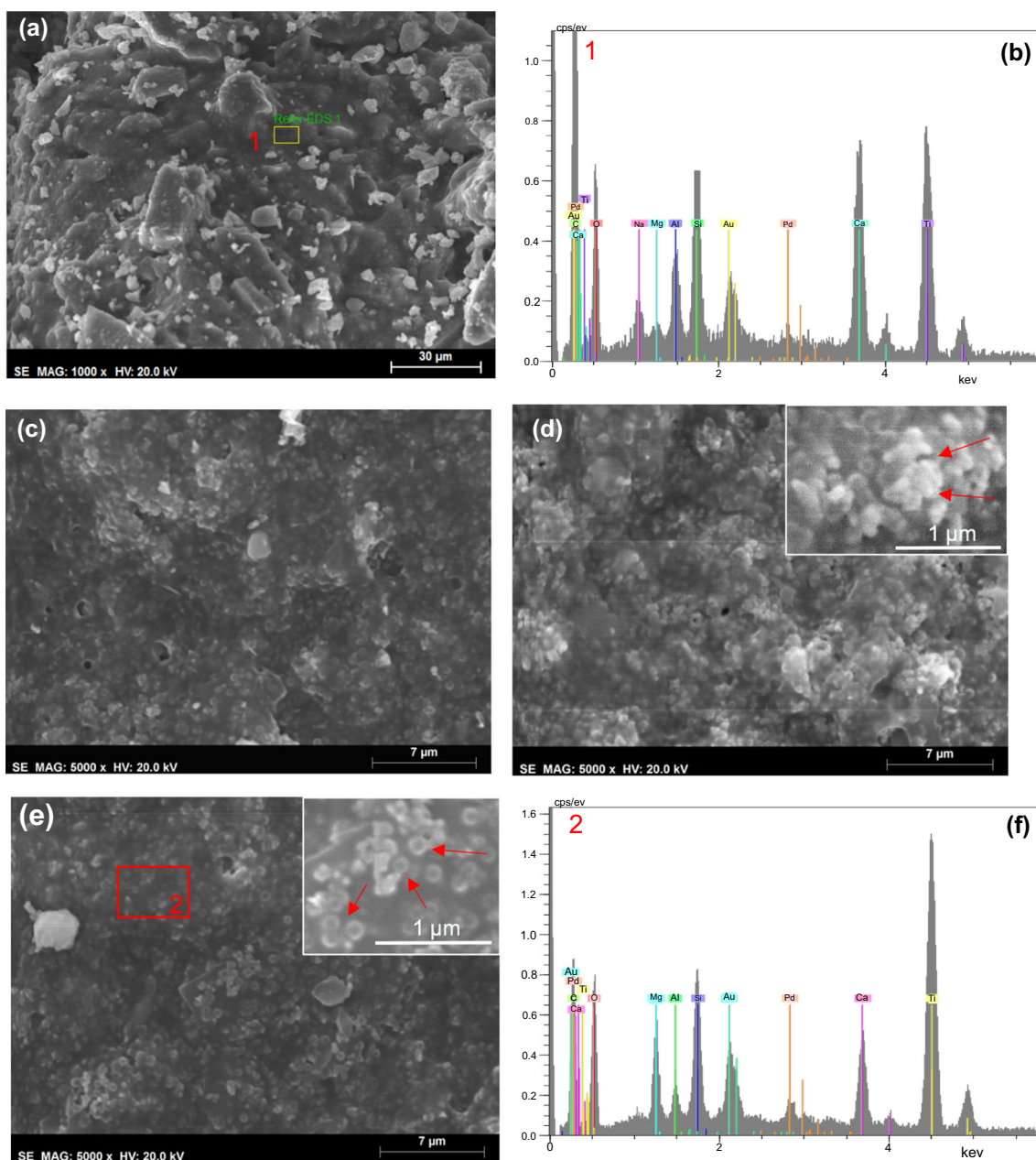


Fig. 4: SEM microphotographs of (a) untreated system and (b) relative EDS elemental map; specimens treated with (c) P1, (d) P2 and (e) P3, and (f) respective EDS map

improved self-cleaning effectiveness of the protective products.

Finally, no noticeable color alterations in the silver chrome aerosol spray stains were observed after sunlight exposure (Fig. 7), as confirmed by the low values of total color variation (lower than 2 units). It seems that the photocatalytic additives cannot interfere in the significant adhesion of the acrylic-based binder (alkyl and polyester resins) of the aerosol silver paint to the substrate.⁴¹

Although the topcoat of the ETICS exhibited considerable photocatalytic properties, the results of

the color variation (ΔE_{ab}^*) confirm that all the three protective products have even higher self-cleaning effectiveness when exposed to solar radiation (Fig. 7a). Color variation values higher than 10 were observed for RhB and MB stains, with P1 and P2 being the specimens with the highest values.⁴² Conversely, $\Delta E_{ab}^* < 2$ was observed in all specimens in the case of the silver aerosol paint, with no visible color changes in this stain.

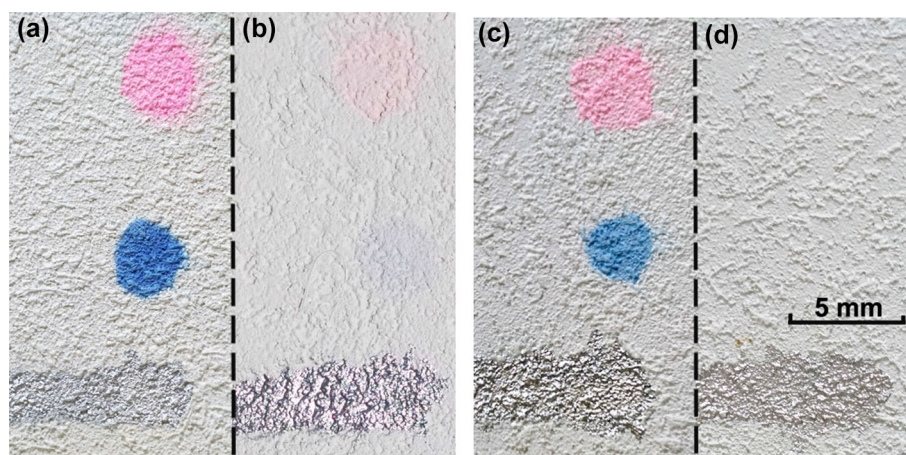


Fig. 5: Stains of rhodamine (RhB, purple), blue methylene (MB), and silver aerosol spray paint (G) in the untreated (P0) and treated (P2) ETICS specimens: (a,c) prior to exposure; (b,d) after 144-168 h of sunlight exposure

Discussion

Results showed that the compactness and mechanical performance (i.e., propagation of ultrasound P-Wave and surface hardness) increased after the application of the protective coatings, with partial filling of the microporous network of the finishing coat. Furthermore, the application of the protective products slightly increased the specular gloss and simultaneously reduced the surface roughness (Fig. 8), in agreement with previous results.⁶ Thus, these products can slightly improve the aesthetic features of the ETICS, as well as arguably reduce the accumulation of aerosol particle and particulate matter by providing a less porous, more compact, and homogeneous surface.

Regarding the contact angle, it was observed that P3 has higher θ , thus this protective coating provided a more hydrophobic treatment,³³ whereas P1 and P2 contribute to a higher (photoinduced) hydrophilicity and wetting capacity of the treated surfaces. Interestingly, it can be observed that θ values are inversely proportional to the color variation (ΔE_{ab}^*) with sunlight exposure, where lower hydrophobicity corresponds to higher color variation, as in the case of P1 and P2 (Fig. 9). The presence of TiO₂ nanoparticles (with both hydrophilic and photocatalytic properties) possibly contributed to this process. It can be concluded that the higher the surface wetting, the most significant the self-cleaning efficacy, in accordance with Saini et al.⁴³

The addition of TiO₂ provides higher self-cleaning properties, which can prevent the deposition of dust, particulate matter and pollutants on the treated substrate. TiO₂ nanoparticles can also efficiently decompose volatile organic compounds (VOCs) and biological macromolecules (DNA),⁴⁴ thus providing a further biocide effect. Additionally, it was reported that TiO₂ nanoparticle (both in the anatase and rutile crystal forms) have unique amphiphilic (both hydrophilic and oleophilic) properties, based on their pho-

tocatalysis activation. In fact, the exposure to a light source substantially decreased the contact angle, and possibly led to superhydrophilic properties ($\theta < 10^\circ$).⁴⁵ The photoinduced hydrophilicity of TiO₂ can facilitate the sheeting and thus removal of water, which can carry away the particle matter accumulated on the substrate.

It is worth noting that high amphiphilicity was repeatedly regenerated by light irradiation, although a storage period in the dark induced a gradual increase in the water-contact angle, revealing a surface wettability trend toward hydrophobicity.⁴¹ Thus, it is arguable that the effectiveness of the TiO₂-enriched coatings would decrease their self-cleaning effectiveness over time, raising doubts on the long-term durability and effectiveness of the protection products. The tendency to the formation of non-photocatalytic hydrophilic surfaces, associated with the leaching or degradation of the biocide,⁴⁶ can also lead to a significant biological susceptibility of the coatings. Previous studies^{51, 47, 48} pointed out that the photoinduced hydrophilicity and self-cleaning effectiveness of treatment with nano-engineered TiO₂ can be partially reduced by weathering; these authors reported that the photoactivity of TiO₂ identified the loss of photocatalytic effectiveness to long-run exposure to UV-A radiation. Additionally, TiO₂ particles are usually encapsulated in hydrous oxides (e.g., SiO₂, Al₂O₃, or ZrO₂ as shell materials) to prevent the contact between the degradable organics (which can lead to discoloration, loss of gloss, or chalking coatings) and the photoactive TiO₂ surface, with the aim of suppressing the TiO₂ photoactivity and improving the resistance to weathering.⁴⁹ A poor encapsulation or the weathering of the shell material might be detrimental to the durability of the treatment, since the TiO₂ might attack the organic-based compounds of the paint (e.g., acrylic-based paint binder).

It is verified that the self-cleaning capability of the three products worked properly outdoors with direct

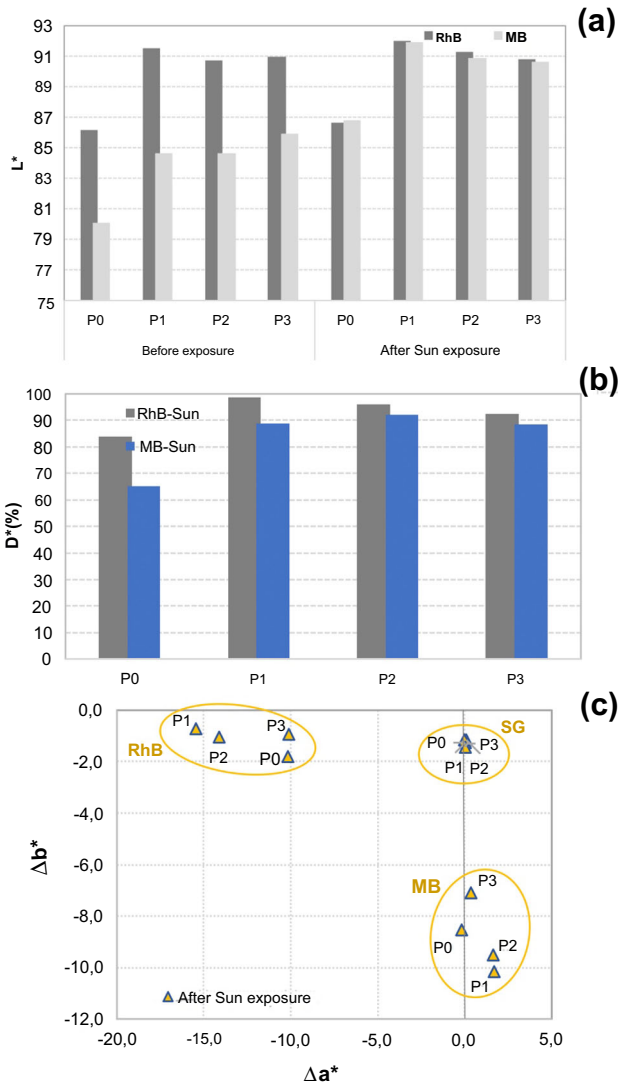


Fig. 6: (a) Average values of lightness (L*) and (b) photocatalytic decoloration of the stains (D*) of rhodamine B (RhB) and methylene blue (MB) for treated and untreated ETICS specimens, prior and after sunlight exposure; (c) variation of a* e b* in the specimens after sunlight exposure, in comparison to unexposed specimens (SG: spray graffiti)

sunlight exposure, eliminating RhB and MB stains. It is worth noting that RhB can be degraded by ordinary TiO₂-sensitized photoreaction under UV light illumination ($\lambda = 400\text{-}100\text{ nm}$),^{7, 50} as explained in “Introduction” section. On the other hand, under visible light illumination ($\lambda = 380\text{-}700\text{ nm}$), RhB can also undergo a dye-sensitized photoreaction,⁷ where the organic molecule absorbs visible light photons, with subsequent formation of RhB⁺ molecular ion radicals on the TiO₂ surface and production of O₂⁻. Both radicals are highly reactive leading to the mineralization or degradation of the organic molecule.

High humidity conditions, as generally registered in some periods (e.g., at night time) in the area of Lisbon,

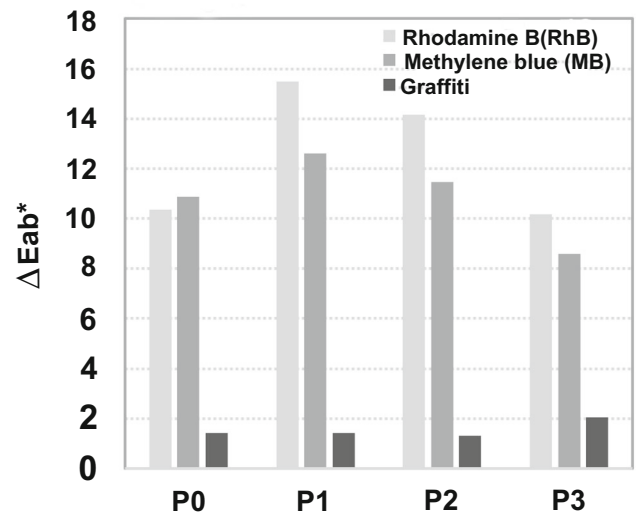


Fig. 7: Color variation (ΔE_{ab}) of rhodamine B (RhB), methylene blue (MB) and silver chrome graffiti after sunlight exposure

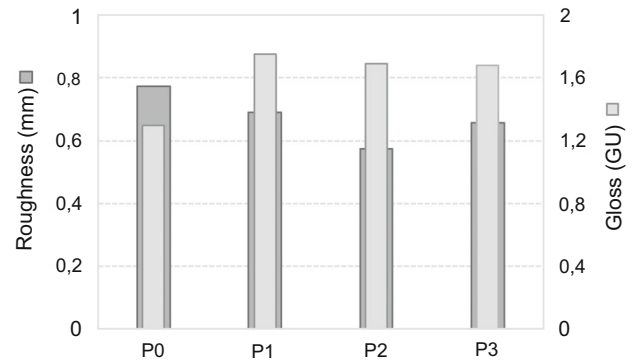


Fig. 8: Roughness and gloss results of treated and untreated specimens

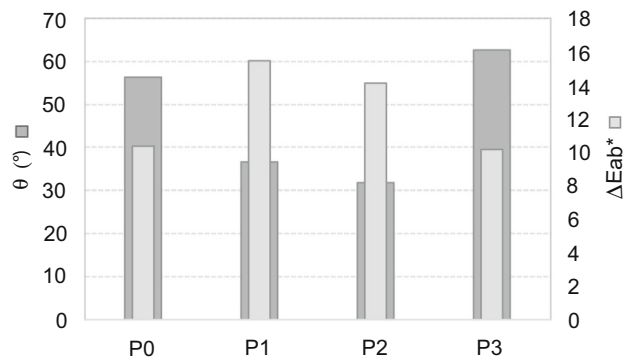


Fig. 9: Variation of the contact angle values (θ) and of the total color variation ΔE^* of treated and untreated specimens after sunlight exposure

even during summer time, might also have favored a more significant photocatalytic effect,^{7, 51–53} and thus removal of the stains in the specimens. Hydrophilic

chemicals (like in the case of MB and RhB) easily form hydrogen bonds with water, and thus photocatalytic water splitting can favor also the removal of this type of hydrophilic materials. Furthermore, ETICS have a high surface condensation potential,⁵⁴ due also to the high vapor resistance of this type of ETICS (with acrylic-based finishing rendering, cementitious base coat and EPS thermal insulation board), which can favor the removal of the water-soluble RhB and MB stains.

Finally, it can be concluded that use of multifunctional products (with hydrophobic, biocide and self-cleaning properties) can be useful for the effectiveness and durability of the ETICS. In fact, hydrophobic features minimize the formation of several ETICS anomalies (e.g., stains, biological growth), and preserve the thermal efficiency of the systems. Furthermore, the self-cleaning effectiveness can help in the minimization of stains of biological origin (e.g., microalgae, cyanobacteria, etc.), as well as in the removal of pollutants and atmospheric particulate matter.⁵⁵ It is worth noting that self-cleaning materials can also replace or partially substitute organic biocide, generally used in acrylic-based paints, which are known to have a relevant impact on the environment and a limited durability over time.⁵⁶

Conclusions

Results show that the three protective coating with self-cleaning and hydrophobic characteristics can provide improved features to the surface of ETICS. In fact, these products enhanced the surface hardness and reduced the porosity on the treated surface. The products have also decreased the surface roughness of the ETICS, preventing the accumulation of undesired particulate matter, and slightly increased the surface gloss, with enhanced aesthetic features. Regarding the self-cleaning effectiveness, which is mainly provided by the addition of photocatalytic additives, i.e., TiO₂ nanoparticles, it was concluded that the three products provided self-cleaning features to the surface after sunlight exposure. A possible contrast among the hydrophobic properties of the acrylic binder or additives, and the amphiphilic features of TiO₂ (which gain superhydrophilic properties under UV irradiation), was also observed.

Based on the results of the color variation, although even the finishing coat of ETICS present photocatalytic properties due to the inclusion of TiO₂ and ZnO, products P1 and P2 had the most significant variations and thus the most efficient self-cleaning effect for the removal of MB and RhB stains. It can be concluded that protective coatings incorporating TiO₂ nanoparticles can effectively induce photo-activated self-cleaning properties, with effective removal of the (rhodamine or methylene blue) stains within 12–14 days of sun exposure. Nevertheless, photocatalytic

additives can not remove the aerosol silver paint, due possibly to the strong adhesion of the acrylic-based binder (alkyl and polyester resins) of the aerosol silver paint to the substrate.

The three protective products are suitable for application on ETICS and can contribute to the long-term performance and durability of these systems. Results suggested that the durability of the ETICS can be enhanced by adopting a properly planned maintenance strategy and periodically applying water-repellent protection products with self-cleaning properties, which can prevent the deposition of particle matter and minimize water penetration and biosusceptibility.

Further studies need to be carried out to evaluate the long-term self-cleaning effectiveness and durability of the TiO₂ paints. Research is on-going with the aim of evaluating the long-term durability of the protective coatings when exposed to an accelerated aging procedure, as well as to evaluate the ecotoxicity and environmental sustainability of the products.

Acknowledgments The authors also acknowledge the company Robbialac for the supply of the products, as well as Pedro Nolasco from NanoMatLab (CQE research unit, IST, Lisbon) for the contact angle measurements.

Funding The authors acknowledge the Portuguese Foundation for Science and Technology (FCT) for funding the research project PTDC/ECI-EGC/30681/2017 (WGB_Shield - Shielding building façades for cities revitalization. Triple resistance to water, graffiti and biocolonization of external thermal insulation systems) and CERIS (UIDB/04625/2020), and the Ph.D. fellowship 2020.05180.BD (J. L. Parracha).

References

1. Tavares, J, Silva, A, De Brito, J, “Computational Models Applied to the Service Life Prediction of External Thermal Insulation Composite Systems (ETICS).” *J. Build. Eng.*, **27** 100944 (2020)
2. Luján, SV, Arrebola, CV, Sánchez, AR, Benito, PA, Cortina, MG, “Experimental Comparative Study of the Thermal Performance of the Façade of a Building Refurbished Using ETICS, and Quantification of Improvements.” *Sustain. Cities Soc.*, **51** 101713 (2019)
3. Edis, E, Türkeri, N, “Durability of External Thermal Insulation Composite Systems in Istanbul Turkey.” *A/Z ITU J. Fac. Archit.*, **9** (1) 134–138 (2012)
4. Amaro, B, Saraiva, D, De Brito, J, Flores-Colen, J, “Statistical Survey of the Pathology, Diagnosis and Rehabilitation of ETICS in Walls.” *J. Civ. Eng. Manag.*, **20** (4) 511–526 (2014)
5. Johansson, S, Wadsö, L, Sandin, K, “Estimation of Mould Growth Levels on Rendered Façades Based on Surface Relative Humidity and Surface Temperature Measurements.” *Build. Environ.*, **45** (5) 1153–1160 (2010)
6. Parracha, JL, Borsoi, G, Flores-Colen, I, Veiga, R, Nunes, L, Dionísio, A, Glória Gomes, M, Faria, P, “Performance

- Parameters of ETICS: Correlating Water Resistance, Bio-Susceptibility and Surface Properties.” *Constr. Build. Mater.*, **272** 121956 (2021)
7. Folli, A, Pade, C, Hansen, TB, De Marco, T, Macphee, DE, “TiO₂ Photocatalysis in Cementitious Systems: Insights into Self-Cleaning and Depollution Chemistry.” *Cem. Concr. Res.*, **42** (3) 539–548 (2012)
 8. Borsoi, G, Esteves, C, Flores-Colen, I, Veiga, R, “Effect of Hygrothermal Aging on Hydrophobic Treatments Applied to Building Exterior Claddings.” *Coatings*, **10** 363 (2020)
 9. Ren, Y, Li, W, Cao, Z, Jiao, Y, Xu, J, Liu, P, Li, S, Li, X, “Robust TiO₂ Nanorods-SiO₂ Core-Shell Coating with High-Performance Self-Cleaning Properties Under Visible Light.” *Appl. Surf. Sci.*, **509** 145377 (2020)
 10. Padmanabhan, NT, John, H, “Titanium Dioxide Based Self-Cleaning Smart Surfaces: A Short Review.” *J. Environ. Chem. Eng.*, **8** 104211 (2020)
 11. Jašková, V, Hochmannová, L, VytLasová, J, “TiO₂ and ZnO Nanoparticles in Photocatalytic and Hygienic Coatings.” *Int. J. Photoenergy*, **795060** 1–6 (2013)
 12. Saad, SR, Mahmed, N, Abdullah, MMAB, Sandu, AV, “Self-Cleaning Technology in Fabric: A Review.” *IOP Conf. Ser. Mater. Sci. Eng.*, **133** 012028 (2016)
 13. Fujishima, A, Rao, TN, Tryk, DA, “Titanium Dioxide Photocatalysis.” *J. Photoch. Photobio. C*, **1** 1–21 (2000)
 14. Bourgeois, PA, Puzenat, E, Peruchon, L, Simonet, F, Chevalier, D, Deflin, E, Brochier, C, Guillard, C, “Characterization of a New Photocatalytic Textile for Formaldehyde Removal from Indoor Air.” *Appl. Catal. B Environ.*, **128** 171–178 (2012)
 15. Lucas, SS, Ferreira, VM, De Aguiar, JB, “Incorporation of Titanium Dioxide Nanoparticles in Mortars—Influence of Microstructure in the Hardened State Properties and Photocatalytic Activity.” *Cem. Concr. Res.*, **43** 112–120 (2013)
 16. Cohen, JD, Sierra-Gallego, G, Tobón, JI, “Evaluation of Photocatalytic Properties of Portland Cement Blended with Titanium Oxynitride (TiO_{2-x}N_y) Nanoparticles.” *Coatings*, **5** (3) 465–476 (2015)
 17. Maury, A, De Belie, N, “State of the art of TiO₂ Containing Cementitious Materials: Self-Cleaning Properties.” *Mater. Constr.*, **60** (298) 33–50 (2010)
 18. Xu, C, Rangaiah, GP, Zhao, XS, “Photocatalytic Degradation of Methylene Blue by Titanium Dioxide: Experimental and Modeling Study.” *Ind. Eng. Chem. Res.*, **53** (38) 14641–14649 (2014)
 19. Krumdieck, SP, Boichot, R, Gorthy, R, Land, JG, Lay, S, Gardecka, AJ, Polson, MI, Wasa, A, Aitken, JE, Heine-mann, JA, Renou, G, “Nanostructured TiO₂ Anatase-Rutile-Carbon Solid Coating with Visible Light Antimicrobial Activity.” *Sci. Rep.*, **9** (1) 1–11 (2019)
 20. Chabas, A, Alfaro, S, Lombardo, T, Verney-Carron, A, Da Silva, E, Triquet, S, Cachier, H, Leroy, E, “Long Term Exposure of Self-Cleaning and Reference Glass in an Urban Environment: A Comparative Assessment.” *Build. Environ.*, **79** 57–65 (2014)
 21. Krishnan, P, Zhang, MH, Yu, L, Feng, H, “Photocatalytic Degradation of Particulate Pollutants and Self-Cleaning Performance of TiO₂-Containing Silicate Coating and Mortar.” *Constr. Build. Mater.*, **44** 309–316 (2013)
 22. Castanho, P, Silva, V, Faria, P, “Assessment of Photocatalytic Capacity of a Hydraulic Mortar.” *41st IAHS WORLD Congr. Innov. Futur.*, Albufeira, PT, September 2016
 23. Guo, MZ, Maury-Ramirez, A, Poon, CS, “Self-Cleaning Ability of Titanium Dioxide Clear Paint Coated Architectural Mortar and Its Potential in Field Application.” *J. Clean. Prod.*, **112** 3583–3588 (2016)
 24. Mendoza, C, Valle, A, Castellote, M, Bahamonde, A, Faraldos, M, “TiO₂ and TiO₂-SiO₂ Coated Cement: Comparison of Mechanic and Photocatalytic Properties.” *Appl. Catal. B Environ.*, **178** 155–164 (2015)
 25. Italian Standardization Authority (Ente Italiano di Normazione - UNI), “Determination of the Photocatalytic Activity of Hydraulic Binders – Rhodamine Method (in Italian).” UNI 11259, Italy, 2008
 26. EOTA, “European Assessment Document EAD 040083-00-0404—External Thermal Insulation Composite Systems (ETICS) with Renderings.” European Organization for Technical Approvals; Brussels, Belgium, 2019
 27. National Laboratory for Civil Engineering (LNEC), “Evaluation of the Mechanical Properties Through Ultrasonic Test – Test Procedure (in Portuguese).” Lisbon, Portugal, LNEC/NRI, Fe Pa 43, 2010
 28. ASTM International, “Standard Test Method for Rubber Property-Durometer Hardness - ASTM D2240.” West Conshohocken, 2015
 29. ASTM International, “Standard Practice for Determination of Graffiti Resistance - ASTM D6578-00.” West Conshohocken, 2000
 30. Rivas, T, Pozo, S, Fiorucci, MP, López, AJ, Ramil, A, “Nd:YVO₄ Laser Removal of Graffiti from Granite. Influence of Paint and Rock Properties on Cleaning Efficacy.” *Appl. Surf. Sci.*, **263** 563–572 (2012)
 31. Munafò, P, Quagliarini, E, Goffredo, GB, Bondioli, F, Licciulli, A, “Durability of Nano-Engineered TiO₂ Self-Cleaning Treatments on Limestone.” *Constr. Build. Mater.*, **65** 218–231 (2014)
 32. Wang, S, Ang, HM, Tade, MO, “Volatile Organic Compounds in Indoor Environment and Photocatalytic Oxidation: State of the Art.” *Environ. Int.*, **33** 694–705 (2007)
 33. Portuguese Institute for the Sea and Atmosphere (Instituto Português do Mar e da Atmosfera – IPMA), <http://www.ipma.pt>
 34. Lerche, CM, Philipsen, PA, Wulf, HC, “UVR: Sun, Lamps, Pigmentation and Vitamin D.” *Photochem. Photobiol. Sci.*, **16** 291–301 (2017)
 35. Vitt, R, Laschewski, G, Bais, AF, Diémoz, H, Fountoulakis, I, Siani, AM, Matzarakis, A, “UV-Index Climatology for Europe Based on Satellite Data.” *Atmosphere*, **11** 727 (2020)
 36. CIE S014-4/E, “Colorimetry Part 4: CIE 1976 L*a*b* Colour Space.” Commission Internationale de l’éclairage, CIE Central Bureau, Vienna, Austria, 2007
 37. Roncon, R, Borsoi, G, Parracha, JL, Flores-Colen, I, Veiga, R, Nunes, L, “Impact of Water-Repellent Products on the Moisture Transport Properties and Mould Susceptibility of External Thermal Insulation Composite Systems.” *Coatings*, **11** 554 (2021)
 38. Koleske, J V, Springate, R, Brezinski, D, Additives Handbook 2011. Paint and Coatings Industry, 2011
 39. Luttrell, T, Halpegamage, S, Tao, J, Kramer, A, Sutter, E, Batzill, M, “Why is Anatase a Better Photocatalyst Than Rutile?—Model Studies on Epitaxial TiO₂ Films.” *Sci. Rep.*, **4** 4043 (2014)
 40. Adelnia, H, Pourmahdian, S, “Soap-Free Emulsion Polymerization of Poly (Methyl Methacrylate-Co-Butyl Acrylate): Effects of Anionic Comonomers and Methanol on the Different Characteristics of the Latexes.” *Colloid. Polym. Sci.*, **292** 197–205 (2014)
 41. Pozo-Antonio, JS, Rivas, T, Jacobs, RMJ, Viles, HA, Carmona-Quiroga, PM, “Effectiveness of Commercial Anti-Graffiti Treatments in Two Granites of Different Texture and Mineralogy.” *Prog. Org. Coat.*, **116** 70–82 (2018)

42. Sharma, G, Wu, W, Dalal, EN, “The CIEDE2000 Color-Difference Formula: Implementation Notes, Supplementary Test Data, and Mathematical Observations.” *Color Res. Appl.*, **30** (1) 21–30 (2004)
43. Saini, A, Arora, I, Ratan, JK, “Photo-Induced Hydrophilicity of Microsized-TiO₂ Based Self-Cleaning Cement.” *Mater. Lett.*, **260** 126888 (2020)
44. Solovyeva, M, Selishchev, D, Cherepanova, S, Stepanov, G, Zhuravlev, E, Richter, V, Kozlov, D, “Self-Cleaning Photoactive Cotton Fabric Modified with Nanocrystalline TiO₂ for Efficient Degradation of Volatile Organic Compounds and DNA Contaminants.” *Chem. Eng. J.*, **388** 1241 (2020)
45. Wang, R, Hashimoto, K, Fujishima, A, Chikuni, M, Kojima, E, Kitamura, A, Shimohigoshi, M, Watanabe, T, “Light-Induced Amphiphilic Surfaces.” *Nature*, **388** 431–432 (1997)
46. Burkhardt, M, Zuleeg, S, Vonbank, R, Schmid, P, Hean, S, Lamani, X, Bester, K, Boller, M, “Leaching of Additives from Construction Materials to Urban Storm Water Run-off.” *Water Sci. Technol.*, **63** (9) 1974–1982 (2011)
47. Calia, A, Lettieri, M, Masieri, M, “Durability Assessment of Nanostructured TiO₂ Coatings Applied on Limestones to Enhance Building Surface with Self-Cleaning Ability.” *Build. Environ.*, **110** 1–10 (2016)
48. Diamanti, MV, Paolini, R, Rossini, M, Basak Aslan, A, Zinzi, M, Poli, T, Pedferri, MP, “Long Term Self-Cleaning and Photocatalytic Performance of Anatase Added Mortars Exposed to the Urban Environment.” *Constr. Build. Mater.*, **96** 270–278 (2015)
49. Guan, R, He, Z, Liu, S, Han, Y, Wang, Q, Cui, W, He, T, “A Novel Photoelectrochemical Approach for Efficient Assessment of TiO₂ Pigments Weatherability.” *Powder Technol.*, **380** 334–340 (2021)
50. Zhang, L, Moralejo, C, Anderson, WA, “A Review of the Influence of Humidity on Photocatalytic Decomposition of Gaseous Pollutants on TiO₂-Based Catalysts.” *Can. J. Chem. Eng.*, **98** (1) 263–273 (2020)
51. Wu, T, Liu, G, Zhao, J, Hidaka, H, Serpone, N, “Photoassisted Degradation of Dye Pollutants. V. Self-Photosensitized Oxidative Transformation of Rhodamine B under Visible Light Irradiation in Aqueous TiO₂ Dispersions.” *J. Phys. Chem. B*, **102** 5845–5851 (1998)
52. Yamamoto, A, Mizuno, Y, Teramura, K, Shishido, T, Tanaka, T, “Effects of Reaction Temperature on the Photocatalytic Activity of Photo-SCR of NO with NH₃ Over a TiO₂ Photocatalyst.” *Catal. Sci. Technol.*, **3** (7) 1771–1775 (2013)
53. Jeong, MG, Park, JE, Seo, HO, Kim, KD, Kim, YD, Lim, DC, “Humidity Effect on Photocatalytic Activity of TiO₂ and Regeneration of Deactivated Photocatalysts.” *Appl. Surf. Sci.*, **271** 164–170 (2013)
54. Barreira, E, Peixoto de Freitas, V, “External Thermal Insulation Composite Systems: Critical Parameters for Surface Hygrothermal Behaviour.” *Adv. Mater. Sci. Eng.*, Article ID 650752 (2014)
55. Dyshlyuk, L, Babich, O, Ivanova, S, Vasilchenko, N, Atuchin, V, Korolkov, I, Russakov, D, Prosekov, A, “Antimicrobial Potential ZnO, TiO₂ and SiO₂ Nanoparticles in Protecting Building Materials from Biodeterioration.” *Int. Biodeterior. Biodegradation*, **146** 104821 (2020)
56. K  uinal, S, Kutti, S, Rauwel, P, Guha, M, Wragg, D, Rauwel, E, “Biocidal Properties Study of Silver Nanoparticles Used for Application in Green Housing.” *Int. Nano Lett.*, **6** 191–197 (2016)

Publisher’s Note Springer Nature remains neutral with regard to jurisdictional claims in published maps and institutional affiliations.